Observation of nonlinear transmission enhancement in cavities filled with nonlinear organic materials

Dan T. Nguyen,[1,*] Chuanxiang Sheng,[1] Jayan Thomas,[1] Robert Norwood,[1] Brian Kimball,[2] Diane M. Steeves,[2] and Nasser Peyghambarian[1]

[1]College of Optical Sciences, University of Arizona, 1630 East University Boulevard, Tucson, Arizona 85721, USA

[2]United States Army Natick Soldier Research Development and Engineering Center, AMSRD-NSR-WS-BN Kansas Street, Natick, Massachusetts 01760-5020, USA

*Corresponding author [redacted]

Received 17 July 2008; accepted 28 August 2008;
posted 25 September 2008 (Doc. ID 98851); published 23 October 2008

We show experimental and theoretical results for enhancement of nonlinear transmission (NT) in moderate finesse cavities filled with nonlinear organic materials (NLOM). Our design for enhancement of nonlinear transmission using micro NLOM cavities compared with reference samples of the same material show that single cavities can enhance the nonlinear response by a factor of 10 or greater under high-absorption conditions. Further enhancement can be achieved in multiple-cavity structures. Other advantages of the cavity structures for nonlinear transmission, such as a higher damage threshold and a broader NT band, are also discussed. Our initial experimental results show a threefold reduction in the nonlinear threshold fluence in a single cavity device compared directly to an identical sample without mirrors, in qualitative agreement with our calculations. © 2008 Optical Society of America

OCIS codes: 190.4360, 190.4400, 140.3360.

1. Introduction

Nonlinear transmission (NT) occurs when the optical transmission through a medium decreases with increasing input intensity. Passive nonlinear transmission is activated by the optical radiation itself and, therefore, can occur without any electronic switches or feedback circuits. The effect has been proven to be effective for the generation of ultrashort pulses [1]. There are various mechanisms for passive nonlinear transmission, such as nonlinear absorption (NLA), nonlinear refraction, and induced scattering. The microscopic origins of these nonlinearities vary widely and include reverse-saturable absorption, two-photon absorption (TPA), optically-induced molecular reorientation in liquid crystals, and the electronic Kerr effect. [2]. Over time, significant effort has been devoted to the investigation of new materials for NT [3–8]. However, the importance of this problem is now driving device engineering as well, in particular the role of new material structures with advanced properties [9–15]. In [13] we proposed a new NT mechanism based on the induced shift of the bandgap of resonant photonic bandgap (RPBG) structures. The advantage of the mechanism is that both nonlinear absorption and nonlinear reflection can occur in the system. The interplay among these two resonances, the optical resonator, and the Bragg resonance in RPBG structures is the origin of both nonlinear absorption and nonlinear reflection. As a result, the NT at the edge of the photonic bandgap (PBG) can be effectively compared with the NT based on the bandgap shift due to the nonlinear refractive index, as proposed in [9]. In general, NT mechanisms based on PBG structures demonstrate very effective nonlinear transmission, but the NT band (the wavelength band in which NT can occur) is quite narrow, since it operates near the edges of the PBG. Moreover, it sets strict conditions on making PBG structures, in general, and RPBGs, in particular. In this paper we propose a design for NT enhancement

0003-6935/08/315777-07$15.00/0
© 2008 Optical Society of America

based on strong resonance of light in microcavities filled with nonlinear absorbers. In Section 2, we experimentally demonstrate threefold reduction in the nonlinear threshold and a very high damage threshold for a single-cavity device compared directly to an identical sample of a 53 μm NLOM with no mirrors. Then, we present theoretically, in Section 3, the advantages of a microcavity for nonlinear transmission compared with a mirrorless sample of material. The simulation results show that enhanced nonlinear response in a single cavity can reach a factor of 10s or greater under high-absorption conditions. Here, we define the enhanced nonlinear transmission in the cavity as the transmission ratio between the mirrorless sample and the cavity under the same conditions. Finally, we discuss more sophisticated designs for even further enhanced nonlinear response and broader NT bands based on multiple-cavity (MC) structures.

The resonant modes of an optical cavity undergo multiple reflection between the two mirrors of the cavity. The energy carried by these modes, and the corresponding light intensities, are strongly enhanced inside the cavity. If the cavity is filled with a nonlinear absorption material (nonlinear absorber) with its absorption region within the resonant modes, the nonlinear absorption will be enhanced due to the high intensity of light inside the cavity. Nonlinear absorption here means that the absorption increases with the light intensity. However, we do not focus on any specific mechanism for nonlinear absorption in this paper. If the system is constructed from multiple cavities, in which different cavities can be filled with different nonlinear absorbers, then the region of absorption enhancement can be widened. Our simulation results also show that the nonlinear enhancement can reach a factor of 100s in a double-cavity structure due to multiple reflections of the resonant modes in the structure. In this paper, we use the transfer matrix method [16–18] to design the dielectric mirrors and to understand qualitatively the properties of a system consisting of multiple cavities.

2. Experiments Demonstrating Nonlinear Enhancement in a Cavity

In this section, we present experimental results that demonstrate reduction in the nonlinear transmission threshold and very high damage threshold for a single-cavity device compared directly to an identical sample without mirrors. Details of our experiments, including the development of the NLOM, will be the subject of a future paper. We developed a nonlinear transmission sample by dissolving a reverse-saturable absorber dye in a low glass transition temperature (T_g) polymer. The RSA dye used was lead (II) tetrakis (4-cumylphenoxy) phthalocyanine (PbTCPc) (Sigma–Aldrich) and the polymer used was poly (acrylic tetraphenyl diaminobiphenylamine) (PATPD) [19] with the plasticizer ethyl carbazole (ECZ). The PATPD-ECZ mixture and PbTCPc were dissolved in a solvent (dichloromethane) with a weight ratio of 99:1 and mixed together by sonicating for 30 min. The solvent was then evaporated off using a rotary evaporator and the resulting material was dried at 35 °C under vacuum for several hours. The solid composite was melt processed between two glass plates with glass spacer beads in between to adjust the thickness to 53 μm. The phthalocyanines exhibit nonlinear transmission at 532 nm (pulsed) via a NLA process. NLA is attributed to a mechanism by which the excited states are populated by a multistep absorption leading to reverse-saturable absorption (RSA). RSA occurs as a result of an intersystem crossing from the lowest excited singlet (S_1) to the lowest triplet state (T_1) and the subsequent population increase during the laser pulse irradiation. The magnitude of the absorption cross section of the triplet-to-triplet transition is in excess of the magnitude of the absorption cross section of the ground to excited state absorption in the singlet level during RSA. This bleaching of the ground singlet level leads to an overall increase in the absorption coefficient due to the incident laser power. The rationale behind selecting substituted lead phthalocyanine is that the spin orbit coupling can enhance the population of the triplet states in lead phthalocyanine due to the heavy metal atom (lead) effect. The heavier the central metal atom, the more probable is the intersystem crossing, which results in a larger population of the triplet state. This will enhance the absorption cross section of the triplet state resulting in enhanced RSA and, hence, improved nonlinear response [20–22]. The Fabry–Perot (FP) cavity was constructed with mirrors having a reflectivity of about 75% at 532 nm and filled with 53 μm of the PATPD/PbTCPc composite.

The nonlinear response was evaluated using a frequency-doubled Nd:YAG laser (532 nm), which provided 5 ns pulse widths at a repetition rate of 1 Hz. We used two polarizers in series to act as an attenuator to adjust the incident laser energy; then the input laser was split into two beams, one of which was employed as a reference while the other was focused onto the films with a 10 cm focal length lens. The incident and transmitted laser energy were collected with a lens and measured simultaneously with two identical photodiodes. Figure 1 shows the nonlinear response characteristics of the two structures under the same conditions.

As can be seen in Fig. 1, the experiment results clearly show a reduction in the nonlinear threshold fluence (defined as the fluence where the transmittance is 50% of linear value) by about a factor of 3, from $\sim$110 mJ/cm^2 in the mirrorless sample to $\sim$40 mJ/cm^2 in the single-cavity sample. Moreover, the damage threshold in the cavity is nearly 4 times higher than that in the sample ($\sim$800 mJ/cm^2 compared with $\sim$225 mJ/cm^2).

Note that the dielectric mirror in our experiments has reflectivity $R \sim 70\%$ at a laser wavelength of 532 nm and that at the level of linear absorption, the total transmission of the cavity in the whole

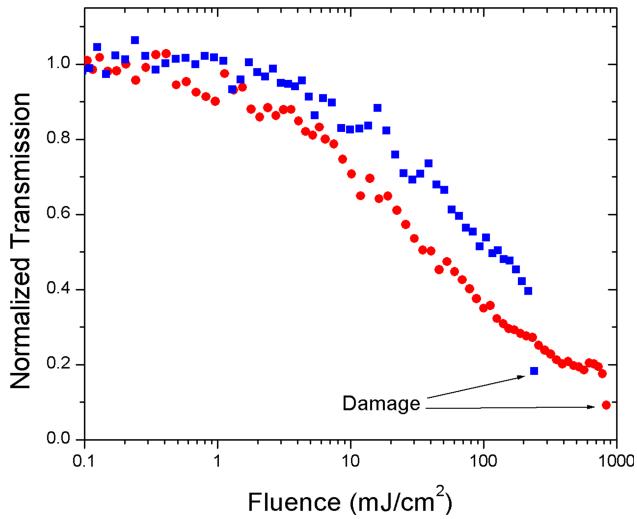

Fig. 1. (Color online) Normalized nonlinear transmission of a single cavity (circles) and a mirorrless sample (squares) of 53 μm of PbPC-doped PATPD. The damage threshold is indicated for both structures.

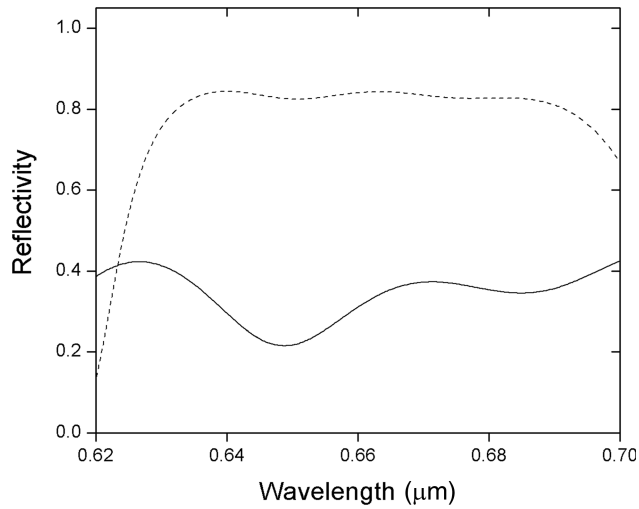

Fig. 2. Mirror reflectivity, M1 (solid curve) and M2 (dashed curve).

visible region (defined as integration of the transmission in the considered region) is about 25%, which is quite low, while the linear transmission in the NT region is only about 10%. Further optimization is required to increase the total linear transmission of the PATPD/PbTCPc FP cavity to a more acceptable level (>30%) while still maintaining the benefits of lower limiting fluence and an increased damage threshold. In principle, we can optimize the mirror to increase the total linear transmission in the visible region to higher than 60%.

3. Theoretical Analysis

In this section, we will present theoretical calculations based on the transfer matrix method (TMM) to understand qualitatively our experiments presented in Section 2. First, let us consider the case of a single cavity (C1), which is constructed from two identical mirrors (M) and is filled with a NLA material characterized by a nonlinear absorption coefficient $\alpha(\lambda)$. Our purpose is to demonstrate the working principle of cavity structures for NT and we do not consider all of the issues related to optimization of the system. The nonlinear enhancement in the cavity, however, strongly depends on the reflectivity of the mirrors and the NLA material. Therefore, we consider two different mirrors, M1 and M2, with $R \sim 40\%$ and $\sim 80\%$, respectively, as shown in Fig. 2.

In our theoretical model and our experimental studies, the dielectric mirrors consist of alternating layers of SiO_2 and Ta_2O_5. In Fig. 2, the reflections of the dielectric mirrors are calculated by the well-known TMM [16]. This method is very effective for calculations of light propagation in multilayer systems, both in frequency [16] and time domains [17,18], so we can apply it to calculate the transmission and reflection of the MC structures. Our calculation method is described as follows.

Let us consider a system, depicted in Fig. 3, consisting of two material layers with different indices n_1 and n_2. $E^{(\pm)}(z)$ denote the electric fields, which propagate forward (+) and backward (−) along the z direction, respectively. $z_m^{\pm} = \lim_{\varepsilon \to 0}(z_m \pm \varepsilon)$ are the right (+) and left (−) boundaries of the coordinates z_m and $d_m = z_m - z_{m-1}$.

The general transfer matrix expression between the fields at z_0 and z_2 can be written as

$$\begin{pmatrix} E^{(+)}(z_0^-) \\ E^{(-)}(z_0^-) \end{pmatrix} = \begin{pmatrix} M_{11} & M_{12} \\ M_{21} & M_{22} \end{pmatrix} \begin{pmatrix} E^{(+)}(z_2^+) \\ E^{(-)}(z_2^+) \end{pmatrix}, \tag{1}$$

where M_{ij} are the coefficients of the transfer matrix M. The electrical field amplitude reflection and transmission are given by

$$\begin{aligned} r &= \left.\frac{E^{(-)}(z_0^+)}{E^{(+)}(z_0^+)}\right|_{E^{(-)}(z_2^+)=0} = \frac{M_{21}}{M_{11}}, \\ t &= \left.\frac{E^{(+)}(z_2^+)}{E^{(+)}(z_0^+)}\right|_{E^{(-)}(z_2^+)=0} = \frac{1}{M_{11}}. \end{aligned} \tag{2}$$

Here, the transfer matrix M can be determined by the simple relations

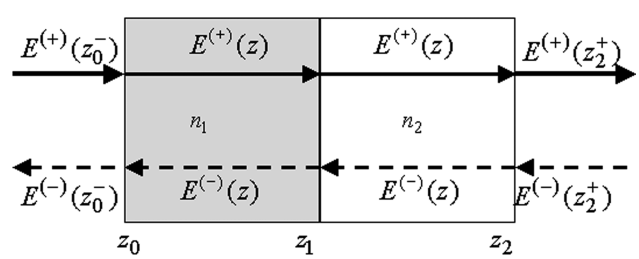

Fig. 3. Scheme for calculation of the light fields by TMM.

$$\begin{pmatrix} E^{(+)}(z_0^-) \\ E^{(-)}(z_0^-) \end{pmatrix} = \frac{1}{2n_0}\begin{pmatrix} n_0+n_1 & n_0-n_1 \\ n_0-n_1 & n_0+n_1 \end{pmatrix}\begin{pmatrix} E^{(+)}(z_0^+) \\ E^{(-)}(z_0^+) \end{pmatrix}$$
$$= \frac{1}{2n_0}\begin{pmatrix} n_0+n_1 & n_0-n_1 \\ n_0-n_1 & n_0+n_1 \end{pmatrix}$$
$$\times \begin{pmatrix} e^{ik_0n_1d_1} & 0 \\ 0 & e^{-ik_0n_1d_1} \end{pmatrix}\begin{pmatrix} E^{(+)}(z_1^-) \\ E^{(-)}(z_1^-) \end{pmatrix}. \quad (3)$$

We define the interface matrix between two adjacent materials as

$$B(n_1|n_r) = \frac{1}{2n_l}\begin{pmatrix} n_l+n_r & n_l-n_r \\ n_l-n_r & n_l+n_r \end{pmatrix}, \quad (4)$$

where n_l and n_r are refractive indices on the left and right of the interface, respectively, and the matrix between two interfaces of a material with thickness d and refractive index n as

$$A(n,d) = \begin{pmatrix} e^{ik_0nd} & 0 \\ 0 & e^{-ik_0nd} \end{pmatrix}, \quad (5)$$

then the transfer matrix equation for the light fields at z_0 and z_2 can be written as

$$\begin{pmatrix} E^{(+)}(z_0^-) \\ E^{(-)}(z_0^-) \end{pmatrix} = B(n_0|n_1)A(n_1,d_1)B(n_1|n_2)$$
$$\times A(n_2,d_2)B(n_2|n_0)\begin{pmatrix} E^{(+)}(z_2^+) \\ E^{(-)}(z_2^+) \end{pmatrix}. \quad (6)$$

Note that in Eqs. (3)–(6), for the case of the absorbing materials, the refractive index is written as $n = n' + in''$, where n' and n'' are the real and imaginary parts of the complex index. The imaginary part of the index is related to the absorption coefficient α_m of the mth layer as $\alpha_m = 2\omega n''_m/c$. By using the above expressions, we can qualitatively calculate light field propagation in single cavities or MC structures, including the multilayer mirrors, in both linear and nonlinear regimes. It is worthwhile stressing that this method gives only qualitative results since it assumes simply that the absorption coefficient $\alpha(\lambda)$ is low in the linear regime (low intensity) and high in the nonlinear regime (high intensity). In this way, the complexity of the nonlinear propagation of the light fields is avoided; however, this method does not fully describe the stronger absorption for resonant modes. It is worth stressing here that the NT of the cavities can be described quantitatively by using the so-called nonlinear transfer matrix formalism (NLTMF) [23,24]. In NLTMF, the nonlinear effects are taken into account in the boundary conditions and in the phases. However, as also presented in [23–25], the NLTMF is essential in cases where the thickness of the nonlinear material is of the order of a wavelength $L \sim \lambda$ and/or in the limit of very high nonlinear refractive index $n_2 I \sim n_0$. In this work, we consider cavities with $L \gg \lambda$ and an NLA material with a negligible nonlinear refractive index. If the nonlinear mechanisms of the materials are known, NT can also be obtained qualitatively by using the time-domain TMM, as in the case of Bragg-space quantum wells [13,17,18]. Here, we consider very general NLA materials, without regard to the particular nonlinear mechanism. The TMM presented above can still describe multiple-reflection effects in the cavities. Therefore, even with such a simple model, we can still demonstrate the advantages of the cavity/MC design for enhanced nonlinear response.

Let us theoretically investigate the advantages of a microcavity for nonlinear transmission. We consider a mirrorless sample C0 and two single cavities (C1s), one with the mirrors M1 (C1M1) and the other with M2 (C1M2). Both cavities and the sample are filled with 200 μm of the same material characterized by the absorption coefficient $\alpha(\lambda)$. For the simplicity of the calculations, we assume that the shape of the absorption spectrum is Lorentzian and is the same in the linear and nonlinear regimes, with only a change in the overall magnitude of the absorption. To illustrate nonlinear enhancement by the cavity structures, we calculate and compare the transmission of the two cavities with that of the mirrorless sample in the linear (low absorption) and nonlinear regimes (high absorption). Figure 4 shows the linear transmissions ($\alpha_{\text{peak}}L = 0.1$ corresponding to $\alpha_{\text{peak}} = 5\,\text{cm}^{-1}$) of C1M2 and mirrorless sample C0.

As seen in Fig. 4, the transmission spectrum of C0 has the oscillations of a microcavity, even though C0 does not have a deposited mirror. This is due to Fresnel reflections at the air/C0 interface where an index of 1.517 is assumed for the C0 system, which is, thus, a weakly resonant cavity itself. It is clear that, in the linear regime (low absorption), mode suppression is relatively weak in these cavities; therefore, the maximum of the linear transmission for both cavities is still relatively high. The linear transmission of C1M1

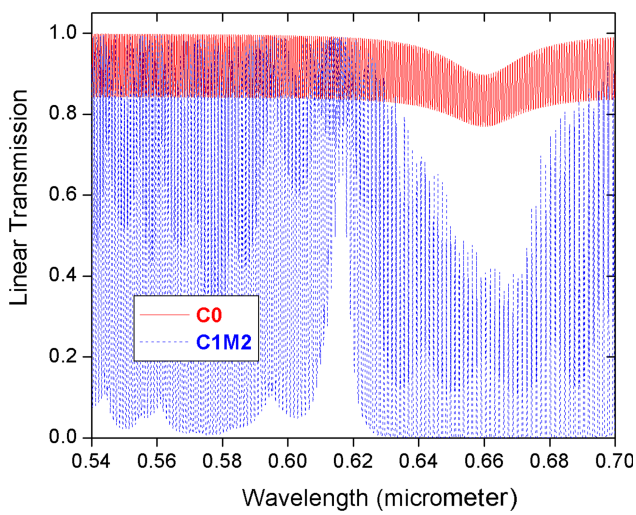

Fig. 4. (Color online) Linear transmission of C0 (solid curve) and C1M2 (dotted curve).

($R \sim 40\%$; not shown here) is higher than that of C1M2 ($R \sim 80\%$) and closer that of C0.

Figure 5 shows the nonlinear transmission of C0, C1M1, and C1M2. Note that all three systems have the same material thickness of 200 μm and are filled with the same absorber with a peak absorption $\alpha_{\text{peak}}L = 2$ at 660 nm ($\alpha_{\text{peak}} = 100\,\text{cm}^{-1}$). Intuitively, if the mirror reflectivity is nearly zero, the cavity behaves like a simple sample without mirrors. Increasing the reflectivity enhances the intensity of the resonant modes inside the cavity. However, if the reflectivity is too high, say nearly 100%, the transmission would be low even in the linear regime. As shown in Fig. 5, the nonlinear enhancement is stronger in C1M2 ($R \sim 80\%$) compared with C1M1 ($R \sim 40\%$). The results show that, with $\alpha_{\text{peak}}L = 2$, the nonlinear enhancement can reach a factor of about 8 in C1M2, and about 2 in C1M1.

The enhancement is even stronger under higher absorption conditions. For example, if $\alpha_{\text{peak}}L = 6$ ($\alpha_{\text{peak}} = 300\,\text{cm}^{-1}$), the nonlinear enhancement in C1M2 can reach a factor of 42 (shown in Fig. 8) and C1M1 a factor of 10. The nonlinear enhancement can be even further increased in MC structures, as will be shown in Section 3. For example, at an absorption peak of $\alpha_{\text{peak}}L$, the nonlinear transmission of a double cavity (C2) is reduced by a factor of more than 300 compared with a mirrorless sample (C0) under the same conditions.

Besides the strong enhancement of the nonlinear effect, i.e., the strong reduction of the nonlinear transmission in cavities as shown in Fig. 5, the damage threshold can be increased significantly in a cavity compared with a mirrorless sample. This results from the reflection or partial reflection of light energy corresponding to nonresonant modes. Thus, the total transmission through the system is reduced significantly compared with a sample without mirrors. The resonant wavelengths undergo multiple reflections inside the cavity and experience enhanced absorption. This is the origin of strong nonlinear enhancement and a higher damage threshold in a cavity. Our experimental results in Section 2 demonstrate reduction in the nonlinear threshold and very high damage threshold for a single-cavity device compared directly with an identical sample without mirrors.

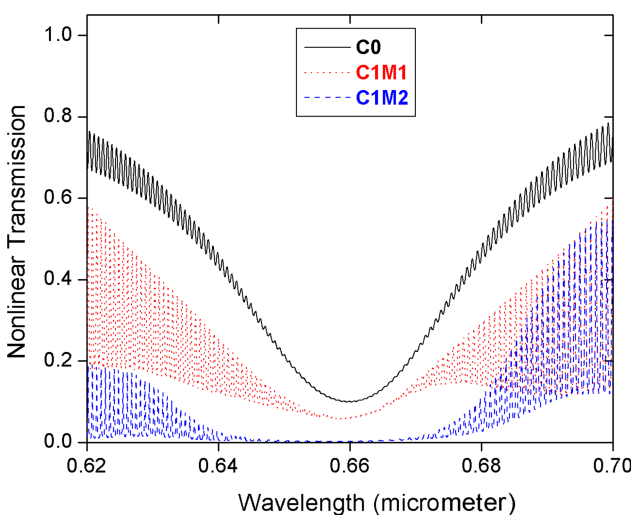

Fig. 5. (Color online) Nonlinear transmission C0 (solid curve), C1M1 (dashed curve), and C1M2 (dotted curve) with peak absorption of $\alpha_{\text{peak}}L = 2$.

We would like to stress here that the results in Figs. 4 and 5 are only qualitative. A full nonlinear analysis would evidence even greater enhancement in the cavity. That is because the results in Figs. 4 and 5 do not reflect the stronger absorption for resonant modes compared with the nonresonant modes inside the cavity. As is well known, the resonant modes (frequencies) of the cavity are the ones that carry most of the light field energy propagating through the system. The nonresonant frequencies get reflected partially and propagate partially through the system. The resonant modes carry much higher energy (stronger intensity) than the nonresonant ones and, therefore, would experience stronger absorption by a nonlinear absorber. However, the transfer matrix method, which is used in our calculations, does not explicitly include the intensity dependence of the absorption coefficient and, as a result, underestimates magnitude of the nonlinear response. The results in Figs. 4 and 5, however, still reflect the fact that resonant light undergoes multiple reflections in a cavity and, therefore, enhances the nonlinear effect compared with a mirrorless sample.

4. Future Directions

In Sections 2 and 3 we have shown, experimentally and theoretically, a strong nonlinear enhancement and an increase of damage threshold in cavities compared with the mirrorless sample of an identical material. A factor of about 42 for nonlinear enhancement can be achieved in a single cavity with the peak absorption $\alpha_{\text{peak}}L = 6$. In this section, we show theoretically that more sophisticated cavity-based structures, i.e., MC structures, can provide more desirable features of nonlinear transmission. Our simulation results show that an MC not only further enhances nonlinear transmission, but can also broaden the NT band by filling the MC with different NLA materials for broadband response in the visible region. Figure 6 shows an MC consisting of six cavities (C6) filled with three different NLA materials. It can also be filled with the same NLA material. We will show numerically that, if an MC is filled with different NLA materials, the NT band can be significantly broadened. On the other hand, an MC with the same NLA

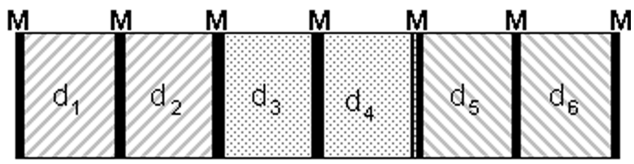

Fig. 6. Sample of multiple cavities structures with six cavities (C6) filled with three different nonlinear absorbers.

material can further enhance the nonlinear response compared with a single cavity, if both systems have the same material length.

Let us consider the case of C6 filled with three NLA materials, which is characterized by three Lorentzian-shaped absorption coefficients $\alpha_i(\lambda)$, $i = 1, 2, 3$, with absorption peaks at 530, 600, and 680 nm, respectively. In Fig. 7, we show the linear (dashed curve) and nonlinear (solid curve) transmission of C6 filled with three nonlinear absorbers, with thickness $d_j = 50$ micron, $j = 1 \div 6$. In the calculations, we assume that, in the linear regime, $\alpha_{i,\mathrm{peak}}L = 0.5$ and, in the nonlinear regime, $\alpha_{i,\mathrm{peak}}L = 5$, where $\alpha_{i,\mathrm{peak}}$ is the absorption peak for material i. It is worth stressing that the NT band of C6 covers a broad overlapping region of three individual bands, while the NT bands of C0 and C1 cover a region corresponding to the absorption band of one material (not shown here). In principle, the number of nonlinear absorbers in the MC structure can further increase, so that the entire visible wavelength region can be covered.

Finally, we compare the nonlinear enhancement in a double cavity and z single cavity in which both systems are constructed with the same mirrors and the same length of the same NLA material. In Fig. 8 we show the calculated nonlinear transmission of a mirrorless sample (C0), a single cavity (C1M2), and a double cavity (C2M2). All three systems have the same length of 200 μm and are filled with the same absorber with the peak absorption at 660 nm. The two cavities have the same mirrors M2 ($R \sim 80\%$).

As can be seen from Fig. 8, the nonlinear enhancement in the double cavity (C2M2) is much stronger than that of a single cavity (C1M2). At an absorption peak of $\alpha_{\mathrm{peak}}L = 6$, the nonlinear transmission of C2M2 is reduced by a factor of about 300, while that of C1M2 has a factor of 42 compared with a mirrorless sample (C0) under the same conditions. In multiple cavities, resonant modes undergo even more reflection inside the system compared with a single cavity. As a result, it can further enhance the nonlinear absorption and, therefore, enhance the nonlinear effects. We would like to stress that, in the linear regime (low absorption), the transmission of the single cavity and double cavity above are comparable.

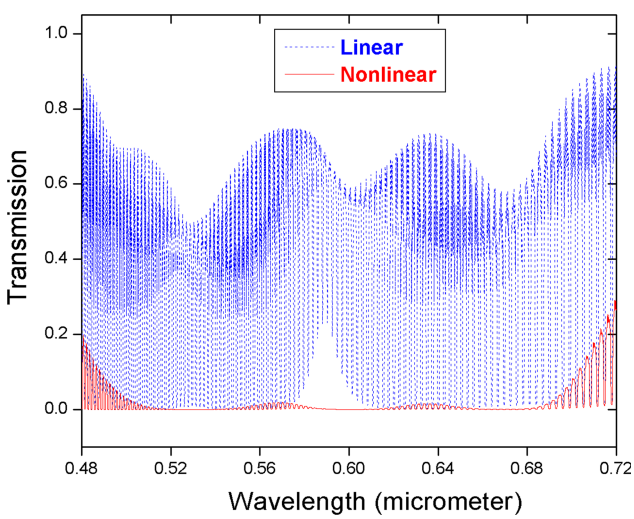

Fig. 7. (Color online) Linear (dotted curve) and nonlinear transmission (solid curve) of C6.

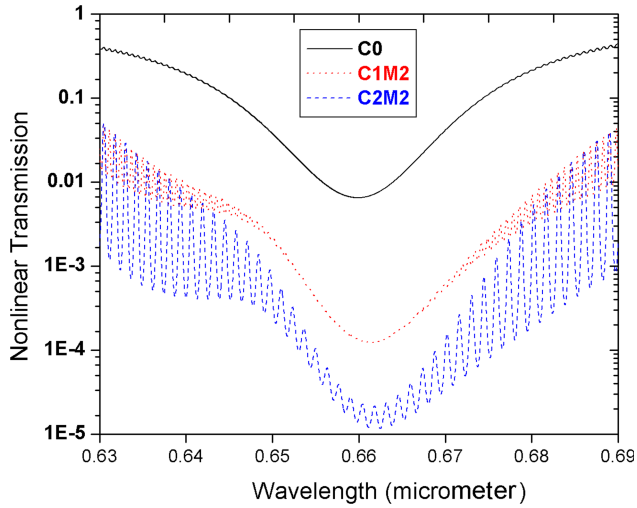

Fig. 8. (Color online) Nonlinear transmission of C1 (solid curve), C1M2 (dashed curve) and C2M2 (dotted curve).

5. Conclusion

We have proposed a new design for enhancement of nonlinear transmission based on cavity structures. Our initial experimental results show a threefold reduction in the nonlinear threshold and a very high damage threshold for a single-cavity device compared directly to an identical sample with no mirrors. We illustrated how MC structures can operate as nonlinear transmission devices to further enhance nonlinear transmission performance and their potential to broaden the nonlinear band. It is worth stressing here that the MC structures are much easier to make than photonic crystal (PC) structures. In MC structures, the thickness of the cavities is not critical and can be much thicker than those in PCs, say, hundreds of micrometers compared with hundreds of nanometers. At the same time, a multiple absorber MC can be easily constructed from the combination of several single absorber cavities, providing the potential for operation over a large wavelength range.

This paper is based upon work supported in part by the United States Army Research Office (USARO) under contract/grant 50372-CH-MUR. We further gratefully acknowledge financial support from the U.S. Army Natick Soldier Research, Development and Engineering Center.

References

1. M. J. Miller, A. G. Mott, and B. P. Ketchel, "General optical limiting requirements," Proc. SPIE **3472**, 24–29 (1998).
2. L. W. Tutt and T. F. Boggess, "A review of optical limiting mechanisms and devices using organics, fullerenes, semiconductors and other materials," Prog. Quantum Electron. **17**, 299–338 (1993).

3. E. W. Van Stryland, Y. Y. Wu, D. J. Hagan, M. J. Soileau, and K. Mansour, "Optical limiting in semiconductors," J. Opt. Soc. Am. B **5**, 1980–1988 (1988).
4. P. Chen, X. Wu, X. Sun, J. Lin, W. Ji, and K. L. Tan, "Electronic structure and optical limiting behavior of carbon nanotubes," Phys. Rev. Lett. **82**, 2548–2551 (1999).
5. M. C. Lacripete, C. Sibillia, S. Paoloni, M. Bertolotti, F. Sarto, and M. Scalora, "Accessing the optical limiting properties of metallo-dielectric photonics band gap structures," J. Appl. Phys. **93**, 5013–5017 (2003).
6. H. Pan, W. Chen, Y. P. Feng, W. Ji, and J. Lin, "Optical limiting properties of metal nanowires," Appl. Phys. Lett. **88**, 223106 (2006).
7. P. Wu, R. Phillip, R. B. Laghumavarapu, J. Devulapalli, D. Rao, B. R. Kimball, M. Nakashima, and B. S. DeCristofano, "Optical power limiting with photoinduced anisotropy of azobenzene films," Appl. Opt. **42**, 4560–4565 (2003).
8. N. Venkatram and D. N. Rao, "Nonlinear absorption, scattering and optical limiting studies of CdS nanoparticles," Opt. Express **13**, 867–872 (2005).
9. M. Scalora, J. P. Dowling, C. M. Bowden, and M. J. Bloemer, "Optical limiting and switching of ultrashort pulses in nonlinear photonic band gap material," Phys. Rev. Lett. **73**, 1368–1371 (1994).
10. B. Y. Soon, J. W. Haus, M. Scalora, and C. Sibilia, "One-dimensional photonic crystal optical limiter," Opt. Express **11**, 2007–2018 (2003).
11. C. Khoo, A. Diaz, and J. Ding, "Nonlinear-absorbing fiber array for large-dynamic-range optical limiting application against intense short laser pulses," J. Opt. Soc. Am. B **21**, 1234–1240 (2004).
12. K. C. Chin, A. Bohel, W. Z. Chen, H. I. Elim, W. Ji, G. L. Chong, C. H. Sow, and A. T. S. Wee, "Gold and silver coated carbon nanotubes: an improved broad-band optical limiter," Chem. Phys. Lett. **409**, 85–88 (2005).
13. D. T. Nguyen, N. H. Kwong, R. Binder, R. Norwood, and N. Peyghambarian, "Optical limiting in Bragg-space quantum wells structures," in *Conference on Laser and Electro-Optics/Quantum Electronics and Laser Science*, Technical Digest (Optical Society of America, 2008), paper JWA18.
14. M. Scalora, N. Mattiucci, G. D'Aguanno, M. Larciprete, and M. J. Bloemer, "Nonlinear pulse propagation in one-dimensional metal-dielectric multilayer stack: ultrawide bandwidth optical limiting," Phys. Rev. E **73**, 016603 (2006).
15. N. N. Lepeshkin, A. Schweinsberg, G. Piredda, R. S. Bennink, and R. Boyd, "Enhancement of the nonlinear optical response of one-dimensional metal-dielectric photonic crystal," Phys. Rev. Lett. **93**, 123902 (2004).
16. P.Yeh, *Optical Waves in Layered Media*, Pure and Applied Optics (Wiley, 1988).
17. D. T. Nguyen, N. H. Kwong, R. Binder, and A. L. Smirl, "Mechanism of all-optical spin-dependent polarization switching in semiconductors quantum well Bragg structures," Appl. Phys. Lett. **90**, 18116 (2007).
18. N. H. Kwong, Z. S. Yang, D. T. Nguyen, R. Binder, and A. L. Smirl, "Light pulse delay in semiconductor quantum well Bragg structures," Proc. SPIE **6130**, 61300A (2006).
19. J. Thomas, C. Fuentes-Hernandez, M. Yamamoto, K. Cammack, K. Matsumoto, G. A. Walker, S. Barlow, B. Kippelen, G. Meredith, S. R. Marder, and N. Peyghambarian, "Bistriarylamine polymer-based composites for photorefractive applications," Adv. Mater. **16**, 2032 (2004).
20. J. S. Shirk, R. G. S. Pong, S. R. Flom, F. J. Bartoli, M. E. Boylez, and A. W. Snow, "Lead phthalocyanine reverse saturable absorption optical limiters," Pure Appl. Opt. **5**, 701–707 (1996).
21. M. Hanack, T. Schneider, M. Barthel, J. S. Shirk, S. R. Flom, and R. G. S. Pong, "Indium phthalocyanines and naphthalocyanines for optical limiting," Coord. Chem. Rev. **219–221**, 235–258 (2001).
22. B. A. Kumar, P. Gopinath, C. P. G. Vallabhan, V. P. N. Nampoori, P. Radhakrishnan, and J. Thomas, "Optical-limiting response of rare-earth metallo-phthalocyanine-doped copolymer matrix," J. Opt. Soc. Am. B **20**, 1486–1490 (2003).
23. J. Danckaert, K. Fobeletes, I. Veretennicoff, G. Vitrant, and R. Reinisch, "Dispersive optical bistability in stratified structures," Phys. Rev. B **44**, 8214–8225 (1991).
24. J. Danckaert, H. Thienpont, I. Veretennicoff, M. Haelterman, and P. Mandel "Self-consistent stationary description of a nonlinear Fabry–Perot," Opt. Commun. **71**, 317–322 (1989).
25. D. Gupta and G. S. Agrawal, "Dispersive bistability in coupled nonlinear Fabry–Perot resonators," J. Opt. Soc. Am. B **4**, 691–695 (1987).